Imaging mass spectrometry involves the direct measurement of the molecular and spatial distribution of hundreds of compounds from a biological tissue and the technique shows immense potential at many stages of the drug discovery process

Keynote review:

Imaging mass spectrometry: fundamentals and applications to drug discovery

Stanislav S. Rubakhin, John C. Jurchen, Eric B. Monroe and Jonathan V. Sweedler

Imaging mass spectrometry (IMS) encompasses a variety of techniques that enable the chemical imaging of analytes, which range in size from atoms and small molecules to intact proteins, directly from biological tissues. IMS is transforming specific areas in biological research with its unique combination of chemical and spatial information. Innovations in instrumentation and imaging protocols will make this approach invaluable at many stages of the drug discovery process, including pharmacological target screening and evaluating the distribution of drug and drug metabolites in cells and tissues. The fundamentals and unique methodology of IMS are discussed, along with exciting new applications to drug discovery science.

Nearly all of the biological processes in the body, including the development of disease and the action of various drugs, involve the interaction and dynamic spatial redistribution of atoms, molecules and molecular complexes. Imaging techniques allow the spatial distribution of specific particles to be mapped. Chemical imaging plays an important role in drug discovery as a screening technique for drug targets and for the assessment of drug distribution inside live or fixed cells, tissues and organs. A battery of imaging methods is used for these tasks, including optical imaging, positron tomography, electron microscopy, atomic force microscopy and scanning tunnel microscopy. These techniques are capable of generating multidimensional pictures with a spatial resolution that can approach the atomic scale and/or femtosecond temporal resolution. However, most of these methods require analyte preselection with labels, affinity tags or expression markers, and therefore produce limited chemical information. The distribution of multiple analytes in biological tissues can be analyzed using infrared and Raman spectroscopy, as well as NMR-based imaging approaches. Although rich in chemical information, these approaches

Stanislav Rubakhin, Jonathan Sweedler, Eric Monroe and **John Jurchen** (left to right) and, in the background, the Beckman Institute, University of Illinois, USA.

The research efforts of our group include the development of new mass spectrometric technologies for the chemical and spatial characterization of cell–cell signaling molecules and the use of these technologies to elucidate the fundamental properties of intercellular signaling in a variety of animal models both normal and pathological. We run the UIUC Neuroproteomics Center on Cell–Cell Signaling, which is supported by the USA National Institute on Drug Abuse. We use several of these techniques to address questions involving changes in the brain during drug escalation and abuse. We have characterized hundreds of novel neuropeptides and neurotransmitters and are incorporating these discoveries into models for prohormone processing. Approaches currently under development for spatial characterization of neuropeptides in the central nervous system by mass spectrometry imaging include: time-of-flight secondary ion mass spectrometry imaging, a 'stretched-sample approach', and measurements of isolated single-cell and subcellular components.

Stanislav S. Rubakhin
John C. Jurchen
Eric B. Monroe
Jonathan V. Sweedler*
University of Illinois,
Urbana,
IL 61801, USA
*e-mail:
sweedler@scs.uiuc.edu

1359-6446/05/$ – see front matter PII: S1359-6446(05)03458-6

GLOSSARY

Imaging MS terminology

Analyte desorption (sputtering): Process whereby molecular fragments, molecules or molecular clusters are removed from a condensed-phase sample into the gas phase. Typically induced by irradiating the sample surface with photons or high-energy particles.
Analyte ionization: Formation of ions from their corresponding neutral analytes by the addition or removal of one or more charged particles, typically protons or electrons.
Desorption electrospray ionization (DESI): Ionization method based on the formation of gaseous analyte ions by the impact of a high-velocity, charged solvent stream onto a sample surface.
Desorption/ionization on silicon (DIOS): Ionization method based on analyte desorption and ionization resulting from the laser irradiation of a specially treated porous silicon surface previously covered with analyte.
Dynamic SIMS: Mode of SIMS occurring when the total primary ion density applied to the sample exceeds ~1×10^{13} primary ions/cm^2 during analysis. Typically used for component analysis and depth profiling.
Electrospray ionization (ESI): Method of generating ions through the production of highly charged solvent droplets, containing dissolved analyte, which yields primarily molecular and often multiply charged ions. The ESI mechanism includes a combination of solvent evaporation, ion desorption and solvent droplet explosion due to coulombic repulsion.
Imaging mass spectrometry (IMS): Mass spectrometric technology enabling the investigation of the chemical profile of a sample surface with spatial resolution and chemical specificity.
Laser desorption ionization (LDI): Ionization method enabling analyte ion generation from untreated sample surfaces on laser irradiation
Matrix-assisted laser desorption/ionization (MALDI) matrix: The matrix promotes the analyte desorption/ionization process on exposure to laser radiation. Typical matrices are small organic molecule with a high absorptivity at a desired laser wavelength.
Mass spectrometer: An instrument capable of ionizing analytes, separating them based on their mass-to-charge ratios, and detecting them to produce a mass spectrum.
Mass spectrometry (MS): Analytical method that measures the mass-to-charge ratios of analyte ions produced by a variety of different ionization approaches.
Mass-to-charge ratio (*m/z*): A value used in mass spectrometry obtained by dividing the mass of an ion or ion cluster (in atomic mass units) by the elementary charge of the ion or ion cluster.
MALDI: An ionization method based on the generation of analyte ions upon laser irradiation of a sample surface containing analyte incorporated into MALDI matrix.
Microprobe: In mass spectrometry, a beam of laser light or charged particles used to induce desorption/ionization of analyte species. In some instances, an entire instrument is called a microprobe.
Microprobe size: The area of a surface sampled by a microprobe in a single measurement/pulse.
Secondary ion mass spectrometry (SIMS): Ionization method using a beam of high-energy ions (primary ions) for sputtering and ionizing analytes (secondary ions).
Static SIMS: A mode of SIMS surface analysis using less than a total primary ion density of ~1×10^{13} primary ions/cm^2 of the investigated sample surface. Typically used for surface profiling and the analysis of molecular ions.
Time-of-flight mass spectrometry (TOF-MS): Mass spectrometry utilizing a mass analyzer in which ions are separated by their *m/z* values according to the length of time they require to traverse a specific distance in a mass spectrometer.

can lack sufficient sensitivity, spatial and chemical resolution for widespread use in the drug discovery process.

The ideal imaging technique should simultaneously detect and identify multiple known and unknown compounds present in biological tissues with at least single-cell spatial resolution. The compounds of interest to researchers vary greatly in size, physicochemical properties, concentration and structure. Furthermore, biological molecules, such as proteins and peptides, can have chiral variability, are present in a variety of different chemical environments in the tissue of a given organism and often undergo conformational changes and post-translational modifications. A chemical imaging approach that can obtain such information has not yet been developed.

Imaging mass spectrometry (IMS; see Glossary for definitions) satisfies many of these challenges. IMS detects the mass of an analyte, this being a universal parameter depending only on the atomic composition of the molecule. In this regard, the labeling of an analyte before the experiment is unnecessary. This enables the detection and imaging of known and unknown analytes without requiring the development of specialized labels, which can be difficult to produce. The isotopic labeling of specific compounds is beneficial to IMS analyses particularly in regard to tracking metabolites but is not necessary in all experiments. Hundreds of compounds can be detected and, in some cases, identified simultaneously with micrometer and even submicrometer spatial resolution in complex biological samples. Additionally, IMS can be used to increase the analytical throughput of repetitive samples such as microarrays and can be automated for the routine comparison of similar samples. Of course, unlike magnetic resonance imaging, IMS cannot easily be used *in vivo* and consumes the sample during analysis.

After a brief outline of several well-established and emerging IMS techniques, the current performance and application of these approaches in various fields of fundamental and applied sciences is presented. Groundbreaking and recent work is emphasized, with a focus on applications relevant to drug discovery and development. More-detailed descriptions of general MS topics including ionization processes, mass analyzers [1,2] and IMS [3–6] are found elsewhere (Box 1).

Fundamentals of imaging mass spectrometry

The main goal of IMS is to use the analytical power of MS to create chemical images illustrating the distribution of both known and unknown molecules in a sample (Figure 1). IMS uses a different set of molecular properties for analyte detection and characterization than approaches based on fluorescence or radioactivity and, as such, is able to observe molecules that are inaccessible to more-traditional imaging techniques. Unknown compounds can be identified and chemically imaged via retrospective analysis of the data obtained from an experiment. A general requirement for mass spectrometric analysis is that the analyte must be transferred from the condensed phase to the gas phase, and then ionized, separated in a vacuum and detected. Thus, IMS differs from many imaging methods in that analyte atoms and molecules are removed from the sample surface during analysis rather than remain in

BOX 1

Key resources	
Online tutorials	
Online mass spectrometry tutorial by Richard Caprioli and Marc Sutter, revised by Markus Stoeckli	www.mc.vanderbilt.edu/msrc/tutorials/index.php
Secondary ion mass spectrometry theory tutorial developed by Ron Fleming of Charles Evans and Associates	www.cea.com/cai/simstheo/caistheo.htm
Essential books	
Gross, M.L. and Caprioli, R.M. (2003) *The Encyclopedia of Mass Spectrometry*, Elsevier Science (www1.elsevier.com/homepage/sal/emas/)	Multi-volume work providing comprehensive coverage of the full range of topics and techniques in the field of mass spectrometry (MS)
Hoffmann, E. *et al.* (1996) *Mass Spectrometry: Principles and Applications*, Wiley; Masson	The principles, theories and key applications of MS are presented
Vickerman, J.C. *et al.* (2001) *ToF-SIMS: Surface Analysis by Mass Spectrometry*, IM; SurfaceSpectra	A comprehensive surveying of the concepts and applications of time-of-flight secondary ion MS
Cole, R.B. (1997) *Electrospray Ionization Mass Spectrometry: Fundamentals, Instrumentation, and Applications*, Wiley	This book presents a wide view of the knowledge of the basic aspects of electrospray ionization (ESI)-MS
Reviews	
Todd, P.J. *et al.* (2001) Organic ion imaging of biological tissue with secondary ion mass spectrometry and matrix-assisted laser desorption/ionization. *J. Mass Spectrom.* 36, 355–369	Review on imaging matrix-assisted laser desorption/ionization (MALDI)-MS
Belu, A.M. *et al.* (2003) Time-of-flight secondary ion mass spectrometry: techniques and applications for the characterization of biomaterial surfaces. *Biomaterials* 24, 3635–3653	Overview of current state of time-of-flight secondary ion mass spectrometry (TOF-SIMS), including imaging applications
Chaurand, P. *et al.* (2004) Proteomics in diagnostic pathology profiling and imaging proteins directly in tissue sections. *Am. J. Pathol.* 165, 1057–1068	Review of state-of-the-art application of MS imaging to diagnostic pathology
Schwartz, S.A. *et al.* (2003) Direct tissue analysis using matrix-assisted laser desorption/ionization mass spectrometry: practical aspects of sample preparation. *J. Mass Spectrom.* 38, 699–708	Description of the actual sample handling procedures for MS imaging
Research groups developing IMS[a]	
The Caprioli research laboratory	www.mc.vanderbilt.edu/msrc/caprioli/index.php
The Cooks group	www.chem.purdue.edu/people/faculty/faculty.asp?itemID=1
The Ewing group	www.chem.psu.edu/profs/Ewing.html
The Heeren group	www.amolf.nl/research/macromolecular_ion_physics/main.html
The National Resource for Imaging Mass Spectrometry at Harvard Medical School	www.nrims.hms.harvard.edu/
The Bioanalytical Laser Mass Spectrometry group headed by Dr Spengler	www.uni-duesseldorf.de/WWW/MedFak/LaserMedizin/pages/massspec.html
The Sweedler group	mrel.beckman.uiuc.edu/sweedler
The Winograd group	nxw.chem.psu.edu/nxw/nxw.asp
Examples of mass spectrometers used in IMS	
Voyager-DE™ STR	MALDI-TOF Workstation includes a linear detection system, a reflecting ion mirror and a collision-induced disassociation cell for enhanced fragmentation in post-source decay analysis. Fully automated acquisition and processing of data (manufacturer– Applied Biosystems, www.appliedbiosystems.com)
QSTAR XL Hybrid LC/MS/MS System	Hybrid Quadrupole Time-of-Flight Mass Spectrometer equipped with advanced MALDI Imaging application software and interchangeable, application-specific ion sources including MALDI source (manufacturer – Applied Biosystems, www.appliedbiosystems.com)
Ultraflex II TOF/TOF MALDI-TOF/TOF	System optimized for the two-dimensional peptide MALDI imaging of cells or tissues, and supported by the flexImaging 1.0 software (manufacturer – Bruker BioSciences Corporation, www.bruker-daltonik.de)
NanoSIMS 50	SIMS Mass Spectrometer capable of image distribution of trace elements and isotopes in tissues, cells and subcellular structures with up to 50 nm spatial resolution. Five or seven masses (ions) can be measured in parallel (manufacturer – CAMECA; www.cameca.fr)
TRIFT IV	TOF-SIMS Mass Spectrometer designed for sub-micron elemental, chemical and molecular characterization and imaging. The instrument can be equipped with liquid metal and Au ion sources (manufacturer – Physical Electronics; www.phi.com)
Miscellaneous	
www.spectroscopynow.com	Comprehensive source of information and internet links on mass spectrometry

[a]Not all groups are listed owing to space limitation.

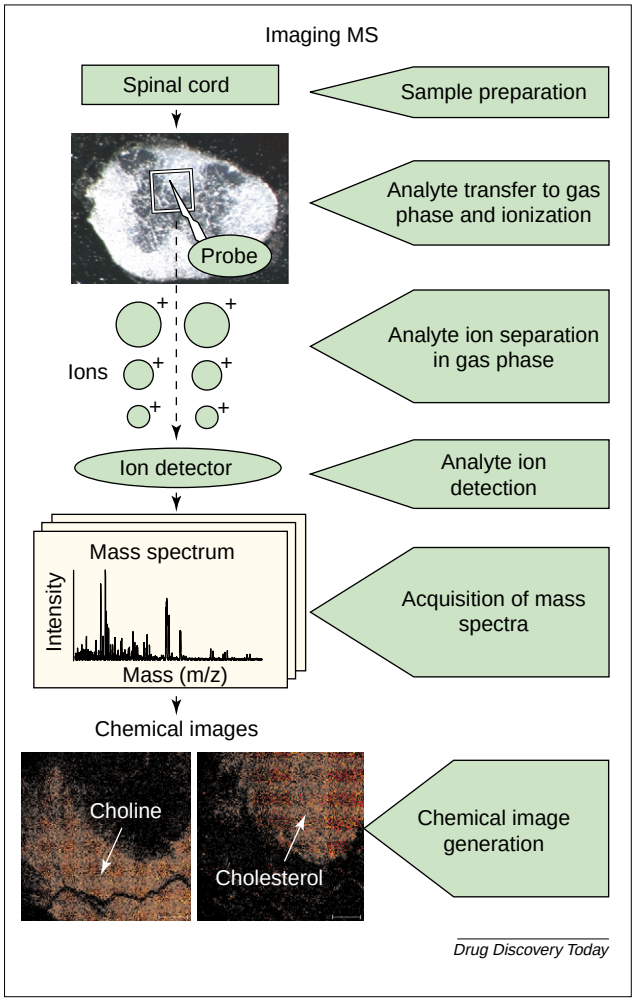

FIGURE 1

The acquisition of chemical images with mass spectrometry involves multiple, often elaborate, steps beginning with sample preparation and ending with the generation of the chemical image. The process of imaging of a spinal cord section using secondary ion mass spectrometry illustrates the processes used for many IMS experiments. The sample preparation step is done outside of the mass spectrometer and consists of spinal cord dissection, freezing, cryostat sectioning, single section deposition on a wafer, and drying. The next three steps are performed inside a TRIFT III time-of-flight secondary ion mass spectrometer (Phi Electronics) equipped with a 22 keV gold ion source (housed at the Center for Microanalysis of Materials, University of Illinois, USA). The primary ion beam, marked on the microphotograph of the spinal cord as Probe (top image), was pulsed at 8 kHz with a 25 ns pulse width and scanned across the sample surface (boxed area) in a 256 point by 256 point raster pattern (resulting in the acquisition of 16384 mass spectra). Unique mass spectra were acquired for each location and stored digitally (the acquisition of mass spectra step). Chemical images were generated by plotting the choline (left bottom image) and cholesterol (right bottom image) signal intensities in 2D space corresponding to the scanned area of the spinal cord section. Ion images of the distribution of multiple analytes can be automatically or manually reconstructed from the set of mass spectra acquired from a sample surface. In this case, the spatial resolution depends on several parameters, including probe size and distance between the analyzed spots.

the sample. Consequently, IMS can be described as a destructive technique; however, in many cases, only a few molecular monolayers of a sample are affected by the analysis, allowing for further studies with the remaining sample.

Two approaches are used in IMS for transferring the analyte to the gas phase. In one approach, laser irradiation or high-energy ion beams are used to desorb analyte particles from the sample surface (Figure 2). The second approach involves the use of electrospray ionization, in which the analyte is introduced into the gas phase and ionized during the evaporation of a highly charged aerosol of a volatile solvent containing the analytes. Furthermore, there are several modes of image acquisition used in IMS. In the first approach, a laser or ion microprobe, typically with micron or submicron dimensions, sequentially analyzes an array of discrete points as the microprobe beam is scanned across the sample surface in a raster pattern. Individual mass spectra are acquired for each point and stored digitally. Specially designed software enables the selection of an analyte signal from the array of mass spectra and plots the intensity of the signal for each individual point in a 2D array. The signal intensity is normally represented by a color scale, thus creating an ion image of analyte distribution. This can be thought of as imaging in a point-by-point manner. In the ion microscope mode (e.g. the camera mode), chemical images are created in manner similar to optical imaging. Unlike optical imaging, which generates an image by detection of photons, IMS uses desorbed (sputtered) ions from the sample. The ions are separated by specialized ion optics that preserve the relative position of these ions in the plane of the sample surface. The ions are detected in a spatially resolved manner and a chemical image is generated. Each of these two IMS approaches produces different types of data and is described in greater detail below.

IMS, with few exceptions, is performed on the same mass spectrometers used for standard MS. Mass spectrometers contain three main components – an ion source, a mass analyzer and an ion detector (Box 2 and Figure 2). Analyte desorption and ionization occur in the ion source. The generated ions are subsequently separated by their mass-to-charge ratio in the mass analyzer and are detected by the ion detector. The performance of the mass spectrometer will depend largely on the type and configuration of each of the three components. The selection of the mass spectrometer used for imaging should be made based on the specific experimental requirements and sample properties.

Three ionization methods have been used in IMS: electrospray ionization (ESI); ion-beam-induced desorption (sputtering) for secondary ion mass spectrometry (SIMS); and laser desorption, including laser desorption/ionization (LDI) and matrix-assisted laser desorption/ionization (MALDI). Secondary ion- and laser desorption/ionization-based IMS are already well-established methods, whereas imaging with ESI sources is a new, promising approach.

Secondary ion mass spectrometry

The development of SIMS began as early as 1910, with the ground-breaking research of Sir Thomson [7]. Arnot and Milligan [8] made key contribution to establishing SIMS

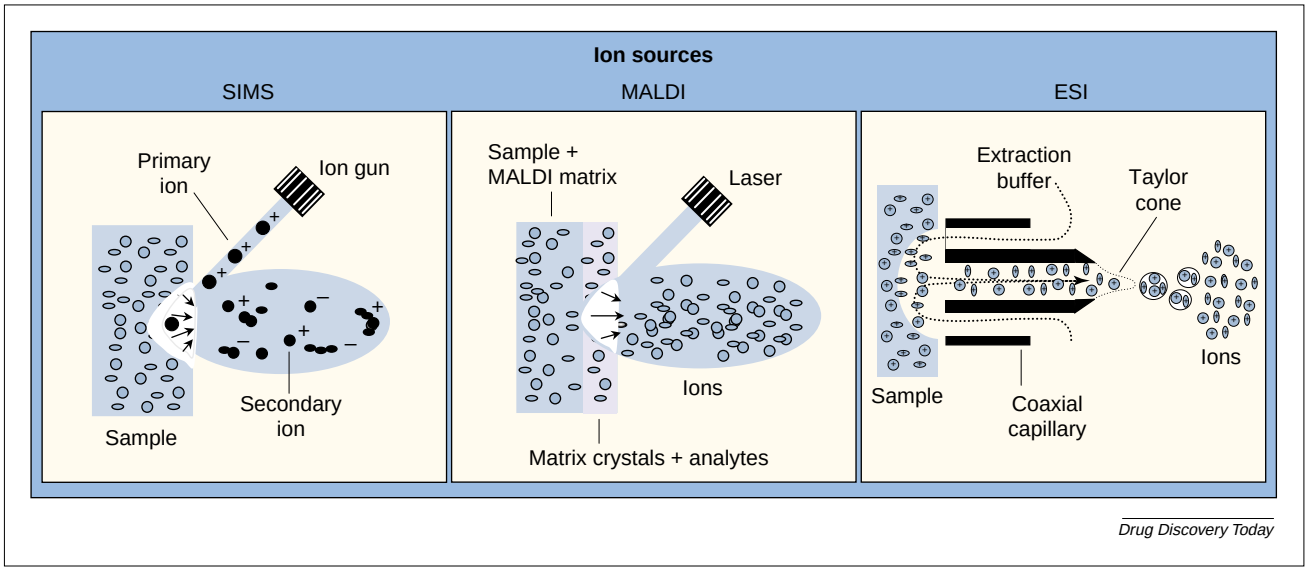

FIGURE 2

Analyte ionization for imaging mass spectrometry occurs in the ion source. Several methods are used in MS to transfer analytes from a condensed-phase sample to the gas phase and to ionize them. For SIMS analysis, a sample surface is irradiated with a beam of primary ions. In MALDI, the sample is irradiated by UV or IR laser pulses. An ESI source forms ions during the evaporation of small, highly charged solvent droplets containing a dissolved analyte.

in 1936. In the early 1960s, Castaing and Slodzian [9] pioneered SIMS-based IMS. More-detailed information on SIMS is available elsewhere [10].

Primary ion sources for SIMS require high vacuum conditions (<10^{-6} torr) and typically use monoatomic, polyatomic, or cluster ion beams having energies in the keV to MeV regime (Figure 2). A large variety of ions and ion clusters have been used in SIMS, including Ar^+, Xe^+, O_2^+, Cs^+, Au^+, Ga^+, He_3^+, SF_6^+, CO_2^+, $C_2F_6^+$, gold cluster ions and C_{60}^+ (buckminsterfullerene) [11–14]. These primary ions are accelerated and focused by an electric field to form a continuous ion beam that is typically pulsed to produce an ionization event. Depending on the application, the diameter of the ion beam can vary from a few hundred micrometers, as used in the ion microscope, to tens of nanometers for high-resolution microprobe work. On impact with the sample surface, the primary ions induce a chain of binary collisions in which the analyte atoms and molecules located within a few nanometers of the impact point are affected [15]. Some of the analyte atoms and molecules are ejected from the surface of the sample into the gas phase in the form of charged and neutral particles. Gold and C_{60}^+ ion sources represent new developments in SIMS that allow the distribution of significantly larger molecules in tissues to be investigated compared with traditional ion sources.

At an ion dosage of ~1×10^{13} primary ions/cm^2 of sample surface, it is postulated that ~1% of the one or two top layers of the sample surface have been probed by SIMS imaging. This is referred to as the static limit, signifying the ion dosage beyond which further sample interrogation has a high probability of analyzing an altered rather than pristine sample surface. Dynamic SIMS is carried out using ion dosages well beyond the static limit and is used to create 3D images. Depth profiling with 0.1–30.0 nm vertical resolution has been achieved using primary ions such as Ga^+, Cs^+ and O_2^+ [16,17]. However, dynamic SIMS tends to yield only atomic and small fragment ions. Therefore, imaging the distributions of large molecules in biological specimens is typically examined in the static regime.

Sample preparation for SIMS imaging is straightforward for most dry solid materials. The sample must fit inside the mass spectrometer and the surface must be smooth and flat to limit ionization and mass-measurement defects because of topography. Several methods have been developed to prepare samples containing volatile compounds (e.g. hydrated biological specimens) for SIMS imaging. Cryofixation by flash freezing in liquid nitrogen slushed liquid propane at a cooling rate of 5000 K/s preserves analyte spatial localization for even small ions such as sodium and potassium. Frozen samples can be inserted directly into the mass spectrometer using a specialized cold transfer stage and analyzed in a hydrated form at low temperatures. Alternatively, frozen samples can be prepared by freeze-substitution and cryo-embedding in resin, or freeze-fractured by a sandwich technique and freeze-dried at –90°C [18]. The freeze-fracturing approach exposes different cellular regions, including the internal space of the plasma membrane. Freeze-dried cells can also be blotted on a metal surface to form a molecular imprint [19]. Chemical fixation with materials such as glutaraldehyde is used in cases when no relocation of analyte will occur during the procedure [20]. Several additional sample treatment protocols can improve analyte sputtering and ion yields. Deposition of analytes on self-assembled monolayers, mixing with organic matrices [21] and

BOX 2

Mass analyzers

The mass analyzer is an essential part of every mass spectrometer. The primary role of the mass analyzer is to separate atomic, molecular, fragment and cluster ions generated by the ion source by *m/z* using electric and/or magnetic fields [(cyclotron frequency in the case of Fourier transform ion cyclotron resonance (FT-ICR)], thus effectively separating them in space. There are at least four types of mass analyzers used in IMS: TOF, magnetic/electric sector, quadrupole ion trap and FT-ICR (Figure I). TOF and magnetic/electric sector mass analyzers are most commonly used in IMS. FT-ICR has rarely been applied to IMS [99].

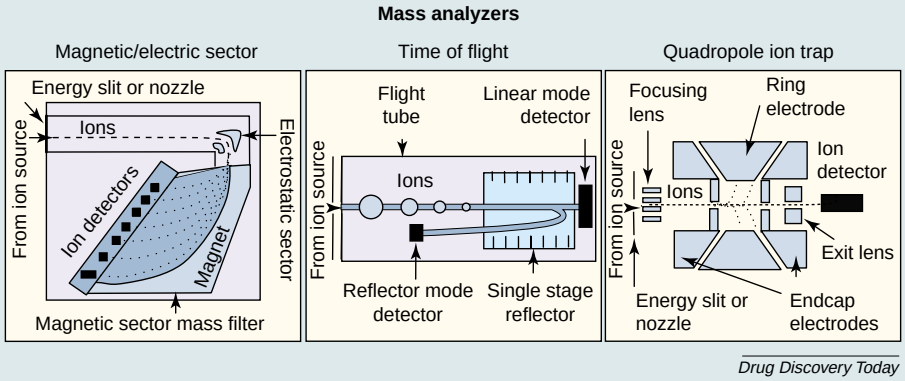

FIGURE I

Mass analyzers employed in IMS research. A schematic representation of the NanoSIMS magnetic/electric sector mass analyzer is depicted on the left panel (www.cameca.fr/html/product_nanosims.html). A TOF mass analyzer is shown in the center panel and illustrates both linear and reflectron modes of operation. A quadrupole ion trap is depicted in the right panel.

Magnetic and electrostatic sector mass analyzers separate ions according to their *m/z* by bending the flight trajectories of the ions with magnetic or electric fields applied perpendicularly to the ion beam path. Ions with larger *m/z* values will be less affected than lighter ions and will follow a longer, shallow trajectory. A single detector at each instrument setting can detect ions with only one *m/z* value and must be adjusted for detection of multiple analyte signals.

The TOF mass analyzer is the fastest, has a broad *m/z* range, is one of most sensitive MS analyzers available and is well-suited to imaging applications. In TOF mass analysis, gas-phase ions produced by a pulsed ion source are accelerated in high vacuum by an electric field. After this acceleration, the ions enter a field-free region between the ion source and detector at a velocity related to their *m/z* with lower *m/z* ions reaching the detector earlier than higher *m/z* ions.

In 3D quadrupole ion trap mass analyzers, radio frequency (RF) voltages are applied to the ring electrode. The endcap electrodes are typically kept at ground potential. Ions with an *m/z* above a selected value are trapped inside the mass analyzer. A continual increase in the RF amplitude applied to the ring electrode results in the ejection of ions passing through an opening in one of the endcap electrodes, towards an ion detector, with ions having a smaller *m/z* being ejected and detected first.

depositing a thin layer of metal onto the sample surface [22] are among such approaches. Artificial components can be added to samples to serve as internal mass calibrants or to allow quantitative or semi-quantitative measurements to be performed. Although useful for relatively small molecules, imaging larger organic molecules, such as proteins, with SIMS presents significant challenges.

Laser desorption/ionization

Besides ions, photons are commonly used to desorb and ionize molecules by LDI. Laser microprobe MS has been in existence for 50 years and offers impressive figures of merit [23,24]. By carefully focusing the laser to the diffraction limit, the spatial resolution can be as high as ~0.5 μm [25]. A commercial instrument utilizing LDI, the laser microprobe mass spectrometer (LAMMA), has been used to image several samples including biological tissues. The desorption process from direct LDI causes molecular fragmentation for most larger organic ions, and so the approach is typically limited to compounds of less than 300 Da, although detection of molecules up to 7000 Da have been reported [26]. For biological samples, this approach is well-suited to elemental composition studies such as locating and measuring transition metals in tissues with sensitivity down to the parts per million level and submicron spatial resolution [27,28].

Matrix-assisted laserdesorption/ionization

One limitation of the primary ion and LDI approaches is that higher molecular weight compounds typically do not survive the desorption process. The ability to characterize biopolymers such as proteins is crucial for understanding many fundamental processes that occur within a living organism. MALDI, introduced by Karas and Hillenkamp [29] and Tanaka *et al.* [30] in the second half of the 1980s, is one of the most powerful methods used to ionize intact biological molecules. In MALDI-MS, the analyte is incorporated into a low-molecular-weight organic matrix, which absorbs the laser radiation (Figure 2). A variety of liquid and solid matrices have been introduced including glycerol, and derivatives of benzoic and cinnamic acids. Not surprisingly, some matrices are more effective at ionizing peptides and proteins whereas others are well-suited to oligonucleotide analysis. MALDI can be performed in a vacuum ($<10^{-6}$ torr) or at atmospheric pressure. Nanosecond UV or IR laser pulses resonantly excite the matrix, causing extremely rapid and localized heating and subsequently the ejection of neutral and charged analyte molecules, matrix molecules and analyte–matrix clusters. Because of particle interactions, analyte ionization occurs in the MALDI matrix crystals and in the MALDI plume. As a result, in positive ionization mode, when the sample is kept on a positively charged metal substrate, mostly monoprotonated $[M + H]^+$ species are formed. The opposite is true in negative ionization

mode, where deprotonated $[M - H]^-$ ions are most abundant. Little fragmentation of analyte molecules occurs during the MALDI desorption process, classifying it as a soft desorption/ionization method.

Soon after the development of MALDI, it was adapted to imaging. The development of MALDI-IMS represents a significant advance in the field of MS, and has been pioneered for tissue analysis in the laboratory of Caprioli [31]. In conventional MALDI-IMS, the sample is coated in a layer of MALDI matrix, and mass spectra are acquired by stepping the laser across the sample, typically in a raster pattern. Chemical images of the distribution of one or more analytes characterized by mass-to-charge (m/z) values are then generated [32–34]. Recently, MALDI-IMS in ion microscope mode has also been demonstrated [35]. In many respects, MALDI-IMS is well-suited to biological tissues. The femtomole to zeptomole limits of detection of MALDI-MS are ideal for the measurement of compounds in biological samples, and MALDI matrices can be dissolved in water or water-containing solvents to produce an acidic environment (pH ~2) that prohibits almost all enzymatic activity and promotes the extraction of intact analyte particles.

Since the 1970s, laser desorption instruments capable of obtaining micron spatial resolution have existed, such that much of the development in MALDI-IMS has involved the improvement of sampling and matrix application techniques. Many of the variables of MALDI-MS sample preparation are complex and have led to a proliferation of methods for sample preparation. One of the key limiting factors for MALDI-IMS of tissue samples is the need to apply a MALDI matrix to extract the analyte vertically from the tissue into matrix crystals while avoiding the corresponding horizontal diffusion and analyte redistribution. Various methods of matrix deposition have been used to minimize this limitation. Several approaches for MALDI matrix deposition for IMS of mammalian tissues have been described, including electrospray deposition [31], manual and robotic assisted formation of random or regular arrays of matrix microdroplets, dipping the sample into a matrix solution, dragging droplets across the sample and depositing matrix with a spray nebulizer [36]. Our group has developed several matrix application approaches for the analysis of invertebrate cultured neurons, including micromanipulator-controlled glass micropipette matrix deposition and low-temperature, high-organic solvent matrix application with rapid drying [37].

As each of these methods has advantages and disadvantages, it is often prudent to evaluate multiple approaches for each sample type to determine the most appropriate. Additionally, several crucial factors must be considered and evaluated before starting any series of imaging experiments: (i) the choice of MALDI matrix – different matrices form crystals of different size and geometry, and this can be a limiting factor for high spatial resolution imaging; (ii) the molecular mass of analytes – various matrices perform differently with analytes of high or low mass; (iii) the matrix solvent – the matrix can be dissolved in a variety of solvents depending on the solubility of the analyte; and (iv) the matrix concentration – a proper analyte:matrix ratio is imperative for optimal ionization. Analyte:matrix molar ratios of 1:100 to 1:10,000 are useful in small-peptide and large-protein analysis, with smaller molecules requiring a lower matrix:analyte ratio.

Desorption/ionization on silicon

Introduced in 1999 by Suizdak [38], desorption/ionization on silicon (DIOS) is similar to MALDI. However, rather than organic matrix, a porous silicon substrate facilitates analyte desorption and ionization under laser irradiation. Although the precise mechanism enabling the desorption of higher molecular weight ions is not well understood, several substrate properties such as a high surface area, prompt photoluminescence and thermal characteristics could contribute to this phenomenon. DIOS produces singly protonated and deprotonated analyte ions and associated sodium and potassium adducts. The application of DIOS for IMS has recently been demonstrated [39]. In DIOS-IMS, liquid or wet samples are deposited on porous silicon and are analyzed after a period of drying. Whereas low-mass compounds can be detected because of the elimination of the MALDI matrix background, DIOS has not been demonstrated for the higher molecular weight proteins.

Electrospray ionization

Fenn [40] successfully applied ESI to the study of large organic molecules in the mid 1980s. To the best of our knowledge, the first demonstration of two-dimensional ESI-IMS was presented by Ford and Van Berkel [41] using a surface sampling probe. This work was a logical extension of several other investigations [42–44], and represents an exciting enhancement to IMS.

In ESI, an aerosol of highly charged droplets composed of volatile solvents and analytes is formed in an electric field (Figure 2). These droplets are subsequently reduced in size by a combination of solvent evaporation and coulombic explosions until charged and neutral analyte molecules are ultimately introduced into the gas phase. In practice, a high electric potential (1–4 kV) is applied between an emitter, typically a metal or metal-coated pulled glass capillary filled with analyte solution, and the entrance to a mass analyzer. The first step in the ESI process is the formation of a Taylor cone from which the ESI droplets are emitted. ESI sources operate at atmospheric pressure and, when used to ionize proteins and large peptides, produce primarily multiply charged (multiply protonated or deprotonated) ions, as well as ions with sodium and potassium adducts. The majority of currently available mass analyzers can analyze multiply charged ions as the distribution of m/z seldom exceeds 2500–3000. Collision-induced fragmentation used for MS-based molecule sequencing is also easier to perform with

multiply charged species. Multiple charges on analytes complicate spectral interpretation as a single analyte could be represented by multiple charge states. ESI is a soft ionization method that is characterized by little or no analyte fragmentation.

Sample preparation for ESI-IMS has been described for mapping of *Ilex vomitoria* extracts separated on thin layer chromatography plates. Molecular images were created by sampling the surface of the plate with a moving probe that is continuously perfused with a 1:1 (v/v) methanol:water elution solution (Figure 2). Theoretically, any flat sample could be scanned with this approach. Stable localization of analyte on the surface before and after scanning and adequate solubility of the analyte in the elution solution are required for a sample to be imaged with ESI-MS. Samples with high concentrations of inorganic salts, detergents or non-volatile substances are unlikely to produce a strong MS signal and must be excluded or treated in a manner to reduce their impact.

Recently, Cooks and co-workers introduced a new method called desorption electrospray ionization (DESI) [45], which enables the acquisition of chemical images of untreated surfaces. The method is based on the formation of primarily singly or multiply charged analyte molecular ions following the impact of charged, electrospray droplets of solvent on the surface being analyzed. An electrospray-related ionization mechanism of ion formation in DESI is suspected. Single dimensional profiling of spatial localization of γ-coniceine in a *Conium maculatum* stem was demonstrated, opening a new promising area in IMS. Recently, Van Berkel *et al.* [46] applied DESI for line scanning of thin-layer chromatography plates. The spatial localization of several drugs including acetaminophen and aspirin separated on a normal-phase silica gel TLC plate was demonstrated.

Choosing an imaging mass spectrometry technique

How does one choose the most appropriate MS-based imaging approach? Obviously, the molecules of interest and experimental parameters are crucial, and the approach chosen would depend on the required *m/z* range, sensitivity, selectivity, spatial resolution and mass resolution. Other parameters of importance include the acquisition time, the number of samples, the details of sample preparation, the need for quantitative information and aspects of spectral interpretation. Both instrumentation and sample preparation methods should be taken into account. For example, the ultimate spatial resolution of an imaging technique depends on both the sample preparation protocols and the instrumentation.

Spatial resolution

Since the 1980s, commercial laser desorption instruments have reported micron resolution and many commercial MALDI-MS instruments can routinely obtain 25 μm resolution. More recently, Spengler *et al.* [47] described a specialized instrument for MALDI–LDI-IMS with a maximum spatial resolution of 0.6 μm for red felt tip dye. SIMS-IMS is capable of imaging surfaces with a lateral resolution of ~50 nm [48,49].

As in other imaging techniques, such as electron microscopy, the effective spatial resolution is often less than would be expected considering only the size of the microprobe and the accuracy of the translation stage or microprobe-positioning device, because the spatial resolution of an image often depends on the properties of the particular samples being analyzed. IMS requires sample preparation protocols that avoid analyte redistribution through active means and diffusion. Typically, analyte extraction and incorporation into the MALDI matrix reduces the effective resolution.

The effective spatial resolution of IMS can also be determined by the analyte concentration. Depending on the sensitivity of the mass spectrometer and the properties of the sample, larger molecules, such as proteins, can be profiled in subcellular structures, single cells and small cellular clusters. For example, a single mammalian cell is typically 10 μm in diameter, has a volume of 500 fl and contains approximately 50 pg or 2 fmol of protein [50]. Whereas some proteins are present in the attomole range, enabling detection, others can be expressed in the zeptomole range, which is typically below the detection threshold. In such cases, it might be necessary to decrease the spatial resolution and use a larger microprobe diameter that will sample enough of the surface to surpass the detection threshold of the mass spectrometer. Usually, samples with smaller and more concentrated analyte molecules (e.g. peptidergic vesicles) can be imaged with a spatial resolution limited only by the size of the microprobe, which varies with the IMS approach. For example, liquid metal ion beams used in SIMS imaging can be focused to less than a 100 nm spot, whereas heavier C_{60}^+ probes routinely exceed ~1 μm size. By comparison, MALDI-IMS operates with laser microprobes, which can be downsized to <1 μm [25,47]. However, particularly small microprobes are not typically practical for the detection of larger molecules such as peptides and proteins localized in most biological specimens as the quantity of analyte in the region of the sample that overlaps with the microprobe footprint is often below the detection limit of the MS system. Thus, the highest resolution molecular images have involved standards or samples of high concentration of analyte.

Analyte mass considerations

The molecular masses of the analytes of interest are important in the selection of an imaging method. For example, SIMS can be ideal for detecting atomic ions and small molecular species below ~500 Da. In some cases, when state-of-the-art ion sources are applied, 2–3 kDa species can be imaged. By contrast, MALDI-IMS and ESI-IMS have less-stringent upper-mass-boundary limitations as MALDI

and ESI ionization sources are capable of producing MDa ions including charged virus particles [51] and ~5 MDa fluorescent microspheres [52]. However, MALDI-MS imaging is difficult in the low mass region (<600 Da) because of MALDI matrix ion interference. LDI or DIOS are useful in this mass range.

Quantitation

Both absolute and relative quantitation with MS is challenging as a result of several factors that influence the intensity of the MS signal. For example, Elsila and co-workers [53] have investigated factors that affect quantitative analysis using microprobe LDI. They found that the validity of quantitative analysis depends on the power and wavelength of the desorption laser, the delay time between the desorption and ionization steps, the power of the ionization laser and the laser alignment. A comparison of time-of-flight (TOF)-SIMS and ^{125}I-radiolabled quantification using a root mean square prediction error method demonstrated that MS data can be significantly influenced by the structure of the adsorbed protein film, the substrate surface chemistry and morphology and the number of latent variables [54]. However, imaging SIMS has demonstrated a linear dependence of analyte signal intensity when normalized to the signal from an internal standard [55]. For direct profiling of biological samples, MALDI-MS is usually a semi-quantitative method. Isotope-coded affinity tag (ICAT) [56] and other isotope-labeling techniques [57] demonstrate the feasibility of relative or absolute analyte quantitation. However, as even a semi-quantitative method, a simple comparison of MS images acquired from two similar samples can produce a wealth of knowledge.

Acquisition time

Image acquisition time must also be taken into account in the selection of an imaging technique (Table 1). The shortest image acquisition time is achieved with imaging SIMS and MALDI-IMS operating in ion microscope mode when a select range of *m/z* is simultaneously recorded over an area. Luxembourg *et al.* [35] reported an acquisition of an image of a peptide distributed on a 200 × 200 μm area in less than 1 ms at a repetition rate of 12 Hz using MALDI-MS as an ion microscope. To date, microscope mode imaging has enabled the collection of data for one *m/z* at a time. A longer time, several hours, is normally required for chemical image generation when operating in microprobe mode where a complete mass spectrum is acquired at each pixel of the image. Even with relatively fast TOF-SIMS imaging, a single scan of a brain slice region of 8 × 8 mm (128 × 128 pixels) with a spatial resolution of 62.5 μm required an acquisition time of 90 min [58]. However, many TOF-SIMS experiments that investigate a smaller surface area can be completed in less than an hour. The differences in acquisition time between ion microscope and microprobe modes might not be so striking when the distribution of multiple substances are examined. When microprobe TOF instruments are used, mass spectra containing multiple analyte signals are acquired at every point of imaged surface. In complex biological samples, hundreds of signals are observed. Thus, to compare the time spent for imaging between microprobe and microscope modes, the total time to generate each of the mass-resolved images should be compared; depending on the number of masses monitored and several other experimental parameters, the overall acquisition time for the two modes of image acquisition can be similar.

A variety of sample preparation methods and IMS techniques allow for the development of an optimal investigative approach to answer various questions that arise in the drug discovery process. In the following section, results obtained using IMS are discussed.

Applications of imaging mass spectrometry

One of the most important steps in drug discovery is the identification of appropriate pharmacological targets. Many diseases have multiple manifestations that include significant changes in biochemical processes and physiological activities. Taking into account the plethora of different and interconnected mechanisms involved in normal and pathological functioning of an organism, how can one determine which particular circuit would best be targeted by a drug? One method to address this question is to screen and compare the biochemistry, physiology and morphology of healthy, diseased and pharmacologically manipulated organs and biological systems using high-throughput methods to attempt to connect measurable changes in chemical abundance to possible cause(s) of disease and response to drug treatment. IMS has been used broadly in such biochemical characterization of cells, and normal and diseased tissues, as well as in the study of fundamental cellular biology.

Imaging cells and tissues

A broad range of chemical species has been investigated using IMS within biological specimens. Low-mass ions such as Na^+, K^+, Ca^{2+}, Cl^- and Br^- derived from biological samples have been investigated using imaging SIMS and can be used to diagnose the physiological state of cells and serve as markers of cellular origin (Table 1). An increased signal for K^+ ions corresponding to a higher K^+ concentration was observed in the interior of a cell, whereas the opposite was found for Na^+ and Ca^{2+} ions [59]. A change in the intensity of the MS signal from inorganic ions might indicate cell damage or the development of pathology such as tumor growth. The accumulation of Cu^+ ions in the cytoplasm of carcinoma PC-3 cells was linked to their increased metastatic potential [60]. Low Ca^{2+} levels were observed in the spindle region of T98G malignant glioma cells during metaphase [61]. Proliferative diabetic retinopathy also demonstrated an increase in the relative intensity of Fe, Ca, Al, Zn and Cu, as well as

TABLE 1

Selected examples of imaging mass spectrometry applications

Substance(s) investigated	Sample (sample preparation method)	Lateral (depth) resolution[a]	Mass range observed as *m/z* (detection limits)	MS imaging method (laser or primary ion source)	Imaging time	Refs
Cholesterol, sulfatides, phosphatidylinositols and phosphatidylcholines	Mouse brain sections (freeze-drying)	~1 μm	800	Static TOF-SIMS (Au_3^+)		[100]
Phospholipids, cholesterol and diglycerides	Mouse brain slices and mouse muscular cells grown onto plastic slips (drying)	427 nm	900	Static TOF-SIMS (Au_1^+, Au_3^+)	1 h 30 min for 64 mm^2 area	[58]
Phosphatidylcholines and 2-aminoethylphosphonolipid	The protozoan *Tetrahymena thermophila* (freeze-fracturing)	250 nm	184	Static TOF-SIMS		[72]
Extract of the caffeine-containing plant *Ilex vomitoria*	C18 thin-layer chromatography plates	77 μm	800 (5 ng)	Ion-trap ESI-MS		[41]
Peptides and proteins	Serial mouse liver and human brain glioma sections of 5–12 μm (snap-freezing, cryostat cutting and thaw-mounting; matrix deposition by discrete droplets or spray-coating)	50 μm	35,000	TOF-MALDI-MS (337 nm)	~2 h for 80 × 96 pixel image	[81]
Proteins	Mouse brain and human glioblastoma xenograft sections (freezing, coating with a solution of matrix)	~25 μm	80,000	TOF-MALDI-MS (337 nm)	42 min for 1000 spot array	[32]
$^{40}Ca^{2+}$, $^{24}Mg^{2+}$, $^{39}K^+$, $^{23}Na^+$, $^{81}Br^-$ and $^{26}CN^-$	Primary fibroblast cells, leukemia progenitor cells and individual chromosomes (cells were cryofixed, cryofractured and dried)	Later ~50 nm, depth ~20 nm steps	81 parts per million	Magnetic sector 3D-SIMS (Ga^+)		[17]
^{12}C, ^{23}Na, ^{24}Mg, ^{39}K, ^{40}Ca, ^{152}Gd, ^{154}Gd, ^{155}Gd, ^{156}Gd, ^{157}Gd, ^{158}Gd, ^{160}Gd and $^{26}(^{12}C^{14}N)$	LLC-PK1 kidney cells, T98G human glioblastoma cells (freeze-fracturing and freeze-drying)	500 nm	160	CAMECA IMS-3f SIMS (O_2^+)	0.4 s for 250 μm^2 image	[16,67,93]
Substance P and β-cyclodextrin	Peptide standards (dried droplet preparation and picospotted samples)	0.6 μm	1384 (800 zmol for β-cyclodextrin)	SMALDI (262 nm and 337 nm)	3–50 min for 100 μm^2 area	[46]
Antitumor drug SCH226374 and compound A	Mouse tumor sections, rat brain sections of 12 μm (freezing, desiccating and drying on MALDI sample plate, spotting or coating with MALDI matrix)	~200 μm		Hybrid quadrupole TOF analyzer MALDI-QqTOF MS (337 nm N_2)	3.5 h for ~17 × 14 mm image	[96]

[a]Maximal lateral resolution presented was measured or estimated.

Abbreviation: SMALDI, scanning microprobe matrix-assisted laser desorption ionization.

vitamin A fragment-1 and palmitic acid ion signals, compared with normal tissue [62]. Submicroscopic localization of potentially toxic In and Al in rat kidney has also been demonstrated [63].

High-resolution SIMS imaging has been applied to the chemical mapping of individual mammalian chromosomes [64], demonstrating the specific binding of Mg^{2+} to the chromosomal 'p' and 'q' arm heterochromatic regions [20]. Quantitative SIMS imaging has provided estimates that one Ca^{2+} ion binds to every 12.5–20 nucleotides and one Mg^{2+} ion binds to every 20–30 nucleotides [17]. Partial decondensation of chromosomes was observed in a low Ca^{2+} and Mg^{2+} environment. During the interphase of the cell cycle, Ca^{2+} and Mg^{2+} were mainly present in the cytosol, whereas both ions were bound to chromatin during metaphase [17]. Imaging SIMS has been used to identify and map DNA localization. The distribution of unlabeled hybridized DNA on peptide nucleic acid (PNA) biosensor chips was imaged by the detection of a phosphorous-containing fragment of the DNA backbone at the complementary PNA positions. [65]. In another research project, phosphate and adenine ions were used as markers of single-strand thiolated oligonucleotide localization on micro-patterned oligonucleotide arrays [66].

An interesting method for mapping amino acids and their metabolites by SIMS imaging was evaluated by Chandra [67]. L-Arginine and phenylalanine, labeled with stable ^{13}C and ^{15}N isotopes, were loaded into cells and the

corresponding $^{28}(^{13}C^{15}N)$ ion signal was detected from different subcellular regions. This demonstrated surprisingly specific localization of elevated amounts of L-arginine-related compounds in nuclei.

The cellular distributions of lipids and lipid fragments, including the head groups of the membrane lipids, have been investigated using TOF-SIMS imaging (Table 1). Studied species include $C_4H_7^+$ at *m/z* 55, phosphocholine head group fragment ions at *m/z* 86 and 184 and ionic fragments of phosphatidylethanolamine at *m/z* 168 and 124 [58,68]. Cholesterol ions (*m/z* 385 for $[M - H]^+$ and *m/z* 369 for $[M - H_2O + H]^+$) and phospholipid ions were detected by SIMS imaging in distinct areas of brain slices rich in cell bodies. In this study, particularly strong cholesterol signals came from morphological structures containing myelinated axons including the corpus callosum, the anterior commissure, the nucleus triangularis septi and the caudate putamen [58,68]. These finding are well corroborated with our observation of the cholesterol distribution in mouse spinal cord (Figure 1). In rat kidney sections, an intense cholesterol signal originated from nuclear areas of epithelial cells and the basal lumina of the renal tubes [69]. Using the molecular imprint-imaging TOF-SIMS method, Sjövall *et al.* [19] demonstrated that phosphocholine is predominantly located in the nuclear membrane, and cholesterol is most abundant in the plasma membrane of blood cells. Probably the first example of lipid imaging in a biological sample with MALDI-MS was presented by Laprevote and co-workers [70]. In this work, differences in lipid composition of regenerated and normal areas of *mdx* mouse leg were observed.

SIMS imaging provides new insights into membrane biochemistry [71]. The mechanisms of membrane fusion of conjugating (mating) protozoan *Tetrahymena* cells were observed by detecting an elevated concentration of the high-curvature lipid 2-aminoethylphosphonolipid in a fusion region [72]. This finding could lead to a better understanding of the mechanisms of many other cellular events such as endocytosis and exocytosis, where highly curved membrane surfaces are typically formed, and demonstrates the ability to use SIMS for measuring dynamic cellular events of interest when determining the function of small molecules on cellular processes.

TOF-SIMS imaging of lipids using polyatomic ion sources (Au_n^+ and C_{60}^+) and an *in situ* freeze-fracture stage was successfully applied to the identification of spores and vegetative cells of the pathogenic bacteria *Bacillus megaterium* by their surface phospholipid 'chemical fingerprints' [73]. The application of traditional MALDI matrices to TOF-SIMS analyses allowed peptides with masses above 2500 Da to be detected and several compounds to be imaged sub-cellularly in the central nervous system [74].

Laser desorption/ionization has been used for several direct imaging experiments of alkali metals, calcium, aluminum, iodine and heavy metals in tissues [27,28]. For example, aluminum and iron have been imaged in neurofibrillary tangles of patients with Alzheimer's disease [75] and the composition of microcalcifications found in rats administered high doses of cyclosporine [28]. Seydel and Lindner [76] have used LAMMA to study the bacterial drug response of intracellular cation content in single cells. A recent study examined the distributions of inhaled carbonaceous compounds in lung tissues [77]. Although the range of compounds measurable by LDI is limited, its impressive imaging performance will ensure its use for selected applications in the drug discovery process.

MALDI-IMS has greatly extended the mass range of IMS, enabling the profiling of peptides and proteins in different biological specimens. Several protocols of sample preparation for IMS have been developed in recent years [36,78]. Using these protocols, molecular ion images of mouse brain [32], human glioma xenografts [32], rat pituitary [31] and mouse epididymis [79] were obtained. In all, more than 400 protein signals have been detected with MALDI-IMS in the 2–100 kDa mass range, with a few hundred signals typically observed in any given 25–100 μm tissue slice region. MALDI-IMS represents a powerful tool for the HTS and discovery of biochemical markers of different diseases including cancer [32,78], Alzheimer's disease [33] and Parkinson's disease [80]. Significant progress towards combining MALDI-IMS with practical clinical use has been made by the development of histological staining protocols compatible with MALDI-IMS, enabling the optical examining and chemical imaging of normal and cancerous tissues [81]. MALDI- and DIOS-MS-based imaging techniques have been used as diagnostic tools for examining the relationships between sample morphology, preparation strategy and spectral quality [34,39], as well as imaging peptide distributions in invertebrate neurons [37] (Figure 3) and an exocrine secretory gland [82].

To date, MALDI-IMS has not been used to acquire protein or peptide sequence information (MS/MS data) over an entire scanned surface, although this powerful identification approach is mainly limited by the properties of the mass spectrometer used and not the ionization method. Thus, in prior work, the identity of proteins has been suggested by matching predicted and measured masses. Data obtained from parallel experiments involving immunostaining, *in situ* hybridization and classical chromatographic or electrophoretic separation followed by protein sequencing assist in peak identification. One possible solution to the protein identification problem is the application of a molecular scanner [83]. The molecular scanner uses enzymes fixed to a semi-permeable membrane to digest proteins from the sample surface. The resulting peptides are then transferred through the membrane onto a collection surface, where they are subsequently subjected to MALDI-IMS and high-throughput protein identification by peptide mass fingerprinting; this has been applied to mouse brain slices [83].

Drug candidate synthesis and screening

Today's drug discovery process is heavily dependent on the synthesis of combinatorial libraries on arrays of polymer resin particles. Because of its specificity, sensitivity, speed, robustness and low sample consumption, IMS is becoming an important analytical tool for screening combinatorial libraries to identify compounds and to determine the purity of the synthesis. TOF-SIMS imaging strategies for the analysis of peptide and non-peptide combinatorial libraries have been developed [84,85]. To optimize MS library screening, several important parameters were evaluated such as linker systems, sample conditioning procedures, linker cleavage and the extraction of unbound analytes. The hydrophilicity of the resin particles was found to be an important factor in preserving analyte spatial localization [86,87]. Recently, progress was achieved in SIMS imaging analysis of combinatorial libraries by applying a new C_{60}^+ ion probe [12,71] that allows the detection of molecules with masses above 600 Da and increases the ion yield by three orders of magnitude over traditional ion sources.

DIOS-MS was also successfully applied to array-based HTS. A set of putative enzyme inhibitors and enzymes with activities similar to phenylalanine hydroxylase (a deficiency of which is a probable cause of phenylketonuria) were investigated [88]. The detection limit of this approach was determined to be 480 peptide molecules [89]. The microfabrication of smaller DIOS sample arrays makes DIOS-IMS a probable candidate for the HTS of combinatorial libraries in the future.

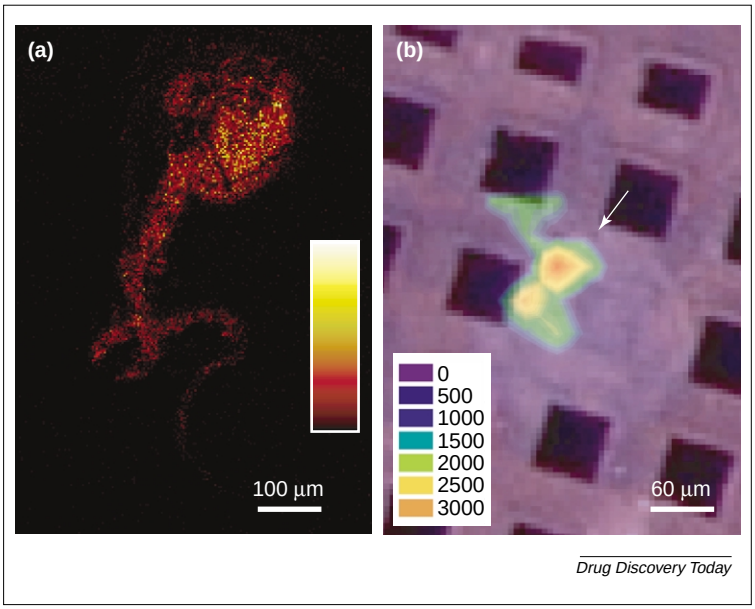

FIGURE 3

Single cell imaging mass spectrometry. (a) SIMS image of the distribution of the phosphatidylcholine lipid head group (*m/z* 184) in a giant molluscan neuron. The image was created at the Center for Microanalysis of Materials using a TRIFT III time-of-flight secondary ion mass spectrometer. **(b)** Overlay of a false-color chemical image of acidic peptide that leaked from a peptidergic neuron and acquired by MALDI-IMS and a photograph of the peptidergic neuron (indicated by white arrows) deposited on a 250 mesh electron microscopy grid and coated with α-cyano-4-hydroxycinnamic acid (HCCA) MALDI matrix. The image was acquired on Voyager DE-STR mass spectrometer (Applied Biosystems) operated in linear mode. Color grids on both images correspond to different signal intensities, with the brightest color indicating the strongest signal.

Drug detection in cells and tissues

IMS has been used intensively to investigate the cellular distribution of well-established and prospective drugs. Chemical maps of the localization of neutron capture therapy (NCT) anticancer drugs such as boron (^{10}B) and gadolinium (^{157}Gd), on a cellular and tissue level, have been created using SIMS imaging. A largely homogeneous distribution of ^{10}B in cytoplasmic and nuclear cellular regions was observed [55,90,91]. However, lower levels of boron were detected in the mitochondria-rich perinuclear cytoplasmic region of individual T98G human malignant glioma cells [92]. The ^{157}Gd signal was localized in the cytoplasmic areas of cultured T98G cells treated with a prospective NCT drug, diethylenetriaminepentaacetic acid GdIII dihydrogen salt hydrate [93]. Fartmann *et al.* [94] presented the quantitative analysis of ^{10}B uptake by human melanoma cells. Using boric acid-doped dextran standards and normalizing the analyte signal intensity to total ion counts, it was estimated that the cells could accumulate 10–30% of the extracellular boron. In a separate research project, a 12-fold increase of ^{10}B accumulation in cancer-affected brain regions was observed [55]. The localization of the β-emitter ^{131}I in different tissues has also been studied with imaging SIMS [20]. Vickerman and co-workers [95] demonstrated that the chlorine-containing antibiotic clofazimine associates with the outer surface of the infectious yeast *Candida glabrata*.

Because of the addition of the matrix, imaging with MALDI-IMS has significant challenges in the detection of low-mass drugs in cells and tissues. This is a result of interference with highly abundant MALDI matrix ions and a lower method sensitivity when using MALDI instruments in reflectron mode as required to distinguish ions with similar *m/z* values [96]. Direct LDI or laser desorption/chemical ionization (LDI/CI) of analytes helps to overcome several of these challenges. However, only a restricted set of small molecules can be analyzed by this method. The distribution of the antipsychotic drug clozapine in rat brain sections was determined using LDI-IMS [68]. LDI/CI-IMS was applied to the analysis of the distribution of spiperone, another antipsychotic drug, in rat liver tissue [97]. MALDI-IMS can be useful in cases of high drug concentration when MALDI matrix signals do not dominate the mass spectra. For example, the distribution of ketoconazole, a component of a medicated shampoo, was visualized in skin with highest concentration in the µg range observed in the dermal skin layer [98]. Several imaging applications for non-TOF mass analyzers were also demonstrated. The anticancer drug paclitaxel was observed in a rat liver and in a human ovarian tumor with a quadrupole (Qq) ion trap mass spectrometer [97]. Recently, Reyzer *et al.* [96] mapped the localization of two

antitumor drug candidates – SCH 226374 and compound A – detecting protonated drug fragments in tissues using a hybrid QqTOF mass spectrometer.

Conclusions

IMS is a rapidly developing field of analytical science, demonstrating promising results in industry and in the fundamental and applied sciences. Determining the spatial distribution of compounds ranging in size from atomic ions to large protein molecules in chromosomes, cells and tissues with micron or even submicron resolution is now feasible with modern IMS. Furthermore, by applying IMS to the screening of combinatorial libraries, the quality and purity of drug candidates can be determined in a high-throughput manner. IMS can be used to develop chemical maps showing the co-localization of drugs with their pharmacological target in cells and tissues with spatial and chemical specificity. Isotopically labeled compounds enable the pinpointing of sites of unusual metabolic activity for further study.

Research in MS is rapidly advancing in areas that include the fundamental investigation of desorption/ionization, analyte identification, quantification, hardware development and its integration into drug research and development. IMS is continually benefiting from progress in these areas. Additionally, IMS is gaining attention as an important technique in its own right, with unique capabilities and requirements. As a result, manufacturers are developing advanced instrumentation for IMS and the academic scientists push the technological boundaries with next generation systems. Special interest lies in the creation of hybrid optical/ion microscopes that will couple histological and mass spectrometric observations. Significant progress in this direction has been demonstrated in recent years. These aspects of scientific development will enable IMS to have an important role in the future of drug discovery and development.

References

1 Benninghoven, A. *et al.* (1988) *Secondary Ion Mass Spectrometry*, Wiley
2 Various (2003) Laser Ablation of Molecular Substrates. *Chem. Rev.* 103, 317–644
3 Sodhi, R.N.S. (2004) Time-of-flight secondary ion mass spectrometry (TOF-SIMS): versatility in chemical and imaging surface analysis. *Analyst* 129, 483–487
4 Todd, P.J. *et al.* (1997) Organic SIMS of biologic tissue. *Anal. Chem.* 69, 529A–535A
5 Pacholski, M.L. and Winograd, N. (1999) Imaging with mass spectrometry. *Chem. Rev.* 99, 2977–3006
6 Winograd, N. (2003) Prospects or imaging TOF-SIMS: from fundamentals to biotechnology. *Appl. Surf. Sci.* 203, 13–19
7 Honig, R.E. (1985) The development of secondary ion mass spectrometry (SIMS): A retrospective. *Int. J. Mass Spectrom. Ion Process.* 66, 31–54
8 Arnot, F.L. and Milligan, J.C. (1936) A new process of negative ion formation. *Proceedings of the Royal Society of London. Series A, Mathematical and Physical Sciences* 156 (889), 538–560
9 Castaing, R. and Slodzian, G. (1962) Microanalyse par emission ionique secondaire. *Microscopie* 1, 395–410
10 Benninghoven, A. *et al.* (1987) *Secondary Ion Mass Spectrometry: Basic Concepts, Instrumental Aspects, Applications, and Trends*, Wiley
11 Tempez, A. *et al.* (2004) Orthogonal time-of-flight secondary ion mass spectrometric analysis of peptides using large gold clusters as primary ions. *Rapid Commun. Mass Spectrom.* 18, 371–376
12 Xu, J. *et al.* (2004) Molecule-specific imaging with mass spectrometry and a buckminsterfullerene probe: application to characterizing solid-phase synthesized combinatorial libraries. *J. Am. Chem. Soc.* 126, 3902–3909
13 Appelhans, A.D. and Delmore, J.E. (1989) Comparison of polyatomic and atomic primary ion beams for secondary ion mass spectrometry of organics. *Anal. Chem.* 61, 1087–1093
14 Hand, O.W. *et al.* (1990) Effects of primary ion polyatomicity and kinetic energy on secondary ion yield and internal energy in SIMS. *Int. J. Mass Spectrom. Ion Process.* 97, 35–45
15 Postawa, Z. (2004) Sputtering simulations of organic overlayers on metal substrates by monoatomic and clusters projectiles. *Appl. Surf. Sci.* 231-2, 22–28
16 Chandra, S. (2004) 3D subcellular SIMS imaging in cryogenically prepared single cells. *Appl. Surf. Sci.* 231-2, 467–469
17 Strick, R. *et al.* (2001) Cation-chromatin binding as shown by ion microscopy is essential for the structural integrity of chromosomes. *J. Cell Biol.* 155, 899–910
18 Chandra, S. and Morrison, G.H. (1992) Sample preparation of animal tissues and cell cultures for secondary ion mass spectrometry (SIMS) microscopy. *Biol. Cell.* 74, 31–42
19 Sjövall, P. *et al.* (2003) Imaging of membrane lipids in single cells by imprint-imaging time-of-flight secondary ion mass spectrometry. *Anal. Chem.* 75, 3429–3434
20 Clerc, J. *et al.* (1997) SIMS microscopy: methodology, problems and perspectives in mapping drugs and nuclear medicine compounds. *Cell Biol. Int.* 21, 619–633
21 Szymczak, W. and Wittmaack, K. (2002) Effect of water treatment on analyte and matrix ion yields in matrix-assisted time-of-flight secondary ion mass spectrometry: the case of insulin in and on hydroxycinnamic acid. *Rapid Commun. Mass Spectrom.* 16, 2025–2033
22 Delcorte, A. *et al.* (2003) Sample metallization for performance improvement in desorption/ionization of kilodalton molecules: quantitative evaluation, imaging secondary ion MS, and laser ablation. *Anal. Chem.* 75, 6875–6885
23 Denoyer, E. *et al.* (1982) Laser microprobe mass spectrometry – 1: Basic principles and performance characteristics. *Anal. Chem.* 54, 26A–41A
24 Hercules, D.M. *et al.* (1982) Laser microprobe mass spectrometry – 1: Basic principles and performance characteristics. *Anal. Chem.* 54, 280A–286A
25 Hillenkamp, F. *et al.* (1975) A high sensitivity laser microprobe mass analyzer. *Applied Physics* 8, 341–348
26 Wilkins, C.L. *et al.* (1985) High mass analysis by laser desorption Fourier transform mass spectrometry. *Anal. Chem.* 57, 520–524
27 Iancu, T.C. *et al.* (1996) The application of laser microprobe mass analysis to the study of biological material. *Biometals* 9, 57–65
28 Verbueken, A.H. *et al.* (1992) Laser microprobe mass spectrometric identification of cyclosporin-induced intrarenal microliths in rat. *Biol. Mass Spectrom.* 21, 590–596
29 Karas, M. and Hillenkamp, F. (1988) Laser Desorption Ionization of Proteins with Molecular Masses Exceeding 10000 Daltons. *Anal. Chem.* 60, 2299–2301
30 Tanaka, K. *et al.* (1988) Protein and polymer analysis up to *m/z* 100.000 by laser ionisation time-of-flight mass spectrometry. *Rapid Commun. Mass Spectrom.* 2, 151–153
31 Caprioli, R.M. *et al.* (1997) Molecular imaging of biological samples: localization of peptides and proteins using MALDI-TOF MS. *Anal. Chem.* 69, 4751–4760
32 Stoeckli, M. *et al.* (2001) Imaging mass spectrometry: a new technology for the analysis of protein expression in mammalian tissues. *Nat. Med.* 7, 493–496
33 Stoeckli, M. *et al.* (2002) Molecular imaging of amyloid beta peptides in mouse brain sections using mass spectrometry. *Anal. Biochem.* 311, 33–39
34 Garden, R.W. and Sweedler, J.V. (2000) Heterogeneity within MALDI samples as revealed by mass spectrometric imaging. *Anal. Chem.* 72, 30–36
35 Luxembourg, S.L. *et al.* (2004) High-spatial resolution mass spectrometric imaging of peptide and protein distributions on a surface. *Anal. Chem.* 76, 5339–5344
36 Schwartz, S.A. *et al.* (2003) Direct tissue analysis using matrix-assisted laser desorption/ionization mass spectrometry: practical aspects of sample preparation. *J. Mass Spectrom.* 38, 699–708
37 Rubakhin, S.S. *et al.* (2003) Spatial profiling with MALDI MS: distribution of neuropeptides within single neurons. *Anal. Chem.* 75, 5374–5380
38 Wei, J. *et al.* (1999) Desorption-ionization mass spectrometry on porous silicon. *Nature* 399, 243–246
39 Kruse, R.A. *et al.* (2001) Experimental factors

controlling analyte ion generation in laser desorption/ionization mass spectrometry on porous silicon. *Anal. Chem.* 73, 3639–3645
40 Fenn, J.B. *et al.* (1989) Electrospray ionization for mass spectrometry of large biomolecules. *Science* 246, 64–71
41 Ford, M.J. and Van Berkel, G.J. (2004) An improved thin-layer chromatography/mass spectrometry coupling using a surface sampling probe electrospray ion trap system. *Rapid Commun. Mass Spectrom.* 18, 1303–1309
42 Modestov, A.D. *et al.* (2001) Scanning capillary microscopy/mass spectrometry for mapping spatial electrochemical activity of electrodes. *Anal. Chem.* 73, 4229–4240
43 Van Berkel, G.J. *et al.* (2002) Thin-layer chromatography and electrospray mass spectrometry coupled using a surface sampling probe. *Anal. Chem.* 74, 6216–6223
44 Wachs, T. and Henion, J. (2001) Electrospray device for coupling microscale separations and other miniaturized devices with electrospray mass spectrometry. *Anal. Chem.* 73, 632–638
45 Takats, Z. *et al.* (2004) Mass spectrometry sampling under ambient conditions with desorption electrospray ionization. *Science* 306, 471–473
46 Van Berkel, G.J. *et al.* (2005) Thin-layer chromatography and mass spectrometry coupled using desorption electrospray ionization. *Anal. Chem.* 77, 1207–1215
47 Spengler, B. and Hubert, M. (2002) Scanning microprobe matrix-assisted laser desorption ionization (SMALDI) mass spectrometry: instrumentation for sub-micrometer resolved LDI and MALDI surface analysis. *J. Am. Soc. Mass Spectrom.* 13, 735–748
48 Guerquin-Kern, J.L. *et al.* (2004) Ultra-structural cell distribution of the melanoma marker iodobenzamide: improved potentiality of SIMS imaging in life sciences. *Biomed. Eng. Online* 3, 10
49 Chabala, J.M. *et al.* (1995) High-resolution chemical imaging with scanning ion probe SIMS. *Int. J. Mass Spectrom. Ion Process.* 143, 191–212
50 Hu, S. *et al.* (2000) Separation of proteins by sodium dodecylsulfate capillary electrophoresis in hydroxypropylcellulose sieving matrix with laser-induced fluorescence detection. *J. Chromatogr. A.* 894, 291–296
51 Bothner, B. and Siuzdak, G. (2004) Electrospray ionization of a whole virus: analyzing mass, structure, and viability. *ChemBioChem* 5, 258–260
52 Cai, Y. *et al.* (2002) Optical detection and charge-state analysis of MALDI-generated particles with molecular masses larger than 5 MDa. *Anal. Chem.* 74, 4434–4440
53 Elsila, J.E. *et al.* (2004) Factors affecting quantitative analysis in laser desorption/laser ionization mass spectrometry. *Anal. Chem.* 76, 2430–2437
54 Wagner, M.S. *et al.* (2003) Quantitative analysis of binary adsorbed protein films by time of flight secondary ion mass spectrometry. *J. Biomed. Mater. Res. A* 64, 1–11
55 Oyedepo, A.C. *et al.* (2004) Analysis of boron-10 in soft tissue by dynamic secondary ion mass spectrometry. *J. Microsc.* 213, 39–45
56 Gygi, S.P. *et al.* (1999) Quantitative analysis of complex protein mixtures using isotope-coded affinity tags. *Nat. Biotechnol.* 17, 994–999
57 Lee, P.J. *et al.* (2004) Qualitative and quantitative analysis of small amine molecules by MALDI-TOF mass spectrometry through charge derivatization. *Anal. Chem.* 76, 4888–4893
58 Touboul, D. *et al.* (2004) Tissue molecular ion imaging by gold cluster ion bombardment. *Anal. Chem.* 76, 1550–1559
59 Chandra, S. (2001) Studies of cell division (mitosis and cytokinesis) by dynamic secondary ion mass spectrometry ion microscopy: LLC-PK1 epithelial cells as a model for subcellular isotopic imaging. *J. Microsc.* 204, 150–165
60 Gazi, E. *et al.* (2004) Imaging ToF-SIMS and synchrotron-based FT-IR micro spectroscopic studies of prostate cancer cell lines. *Appl. Surf. Sci.* 231-2, 452–456
61 Chandra, S. (2003) SIMS ion microscopy as a novel, practical tool for subcellular chemical imaging in cancer research. *Appl. Surf. Sci.* 203, 679–683
62 Kishikawa, Y. *et al.* (2003) Elements and organic substances in epiretinal proliferative tissue excised during vitreous surgery: analysis by time-of-flight secondary-ion mass spectrometry. *J. Electron Microsc. (Tokyo)* 52, 349–354
63 Galle, P. *et al.* (2004) Subcellular localization of aluminum and indium in the rat kidney. *Appl. Surf. Sci.* 231-2, 475–478
64 Levi-Setti, R. *et al.* (1997) Imaging of BrdU-labeled human metaphase chromosomes with a high resolution scanning ion microprobe. *Microsc. Res. Tech.* 36, 301–312
65 Arlinghaus, H.F. *et al.* (2004) Development of PNA microarrays for gene diagnostics with TOF-SIMS. *Appl. Surf. Sci.* 231-2, 392–396
66 Cheran, L.E. *et al.* (2003) Imaging TOF-SIMS analysis of oligonucleotide microarrays. *Analyst* 128, 126–129
67 Chandra, S. (2004) Subcellular SIMS imaging of isotopically labeled amino acids in cryogenically prepared cells. *Appl. Surf. Sci.* 231-2, 462–466
68 Todd, P.J. *et al.* (2001) Organic ion imaging of biological tissue with secondary ion mass spectrometry and matrix-assisted laser desorption/ionization. *J. Mass Spectrom.* 36, 355–369
69 Nygren, H. *et al.* (2004) Bioimaging TOF-SIMS: localization of cholesterol in rat kidney sections. *FEBS Lett.* 566, 291–293
70 Touboul, D. *et al.* (2004) Changes of phospholipid composition within the dystrophic muscle by matrix-assisted laser desorption/ionization mass spectrometry and mass spectrometry imaging. *Eur. J. Mass Spectrom.* 10, 657–664
71 Xu, J. *et al.* (2004) ToF-SIMS imaging with cluster ion beams. *Appl. Surf. Sci.* 231-2, 159–163
72 Ostrowski, S.G. *et al.* (2004) Mass spectrometric imaging of highly curved membranes during tetrahymena mating. *Science* 305, 71–73
73 Thompson, C.E. *et al.* (2004) ToF-SIMS studies as a tool to discriminate between spores and vegetative cells of bacteria. *Appl. Surf. Sci.* 231-2, 420–423
74 Altelaar, A.F. *et al.* (2005) Direct molecular imaging of *Lymnaea stagnalis* nervous tissue at subcellular spatial resolution by mass spectrometry. *Anal. Chem.* 77, 735–741
75 Good, P.F. *et al.* (1992) Selective accumulation of aluminum and iron in the neurofibrillary tangles of Alzheimer's-disease – a laser microprobe (LAMMA) study. *Ann. Neurol.* 31, 286–292
76 Seydel, U. and Lindner, B. (1988) Monitoring of bacterial drug response by mass-spectrometry of single cells. *Biomed. Environ. Mass Spectrom.* 16, 457–459
77 Domej, W. *et al.* (2004) Clinical applicability of mass spectrometry for inhaled carbon compounds and the characterization of trace element patterns in body fluids. *Curr. Pharm. Biotechnol.* 5, 89–106
78 Chaurand, P. *et al.* (2004) Assessing protein patterns in disease using imaging mass spectrometry. *J. Proteome Res.* 3, 245–252
79 Chaurand, P. *et al.* (2003) Profiling and imaging proteins in the mouse epididymis by imaging mass spectrometry. *Proteomics* 3, 2221–2239
80 Pierson, J. *et al.* (2004) Molecular profiling of experimental Parkinson's disease: direct analysis of peptides and proteins on brain tissue sections by MALDI mass spectrometry. *J. Proteome Res.* 3, 289–295
81 Chaurand, P. *et al.* (2004) Integrating histology and imaging mass spectrometry. *Anal. Chem.* 76, 1145–1155
82 Kruse, R. and Sweedler, J.V. (2003) Spatial profiling invertebrate ganglia using MALDI MS. *J. Am. Soc. Mass Spectrom.* 14, 752–759
83 Rohner, T.C. *et al.* (2005) MALDI mass spectrometric imaging of biological tissue sections. *Mech. Ageing Dev.* 126, 177–185
84 Brummel, C.L. *et al.* (1994) A mass spectrometric solution to the address problem of combinatorial libraries. *Science* 264, 399–402
85 Brummel, C.L. *et al.* (1996) Evaluation of mass spectrometric methods applicable to the direct analysis of non-peptide bead-bound combinatorial libraries. *Anal. Chem.* 68, 237–242
86 Xu, J.Y. *et al.* (2003) Applicability of imaging time-of flight secondary ion MS to the characterization of solid-phase synthesized combinatorial libraries. *Anal. Chem.* 75, 6155–6162
87 Xu, J.Y. *et al.* (2003) Rapid screening of molecular arrays using imaging TOF-SIMS. *Appl. Surf. Sci.* 203, 201–204
88 Shen, Z.X. *et al.* (2004) A mass spectrometry plate reader: monitoring enzyme activity and inhibition with a desorption/ionization on silicon (DIOS) platform. *ChemBioChem* 5, 921–927
89 Trauger, S.A. *et al.* (2004) High sensitivity and analyte capture with desorption/ionization mass spectrometry on silylated porous silicon. *Anal. Chem.* 76, 4484–4489
90 Chandra, S. *et al.* (1999) Mapping of intracellular organelles in relation to boron distribution in the same human glioblastoma cell for the evaluation of the efficacy of anticancer boronated drugs. In *Proceedings International Conference Secondary Ion Mass Spectrometry.* (Vol. SIMS, XII), pp. 927–930
91 Bennett, B.D. *et al.* (1994) Subcellular localisation of p-boronophenylalanine-delivered boron-10 in the rat 9L gliosarcoma: cryogenic preparation *in vitro* and *in vivo*. *Radiat. Res.* 140, 72–78
92 Chandra, S. *et al.* (2002) Imaging of fluorine and boron from fluorinated boronophenylalanine in the same cell at organelle resolution by correlative ion microscopy and confocal laser scanning microscopy. *Clin. Cancer Res.* 8, 2675–2683
93 Smith, D.R. *et al.* (2004) Subcellular SIMS imaging of gadolinium isotopes in human glioblastoma cells treated with a gadolinium containing MRI agent. *Appl. Surf. Sci.* 231-2, 457–461
94 Fartmann, M. *et al.* (2004) Quantitative imaging of atomic and molecular species in cancer cultures with TOF-SIMS and Laser-SNMS. *Appl. Surf. Sci.* 231-2, 428–431
95 Cliff, B. *et al.* (2003) Probing cell chemistry with time-of-flight secondary ion mass spectrometry:

development and exploitation of instrumentation for studies of frozen-hydrated biological material. *Rapid Commun. Mass Spectrom.* 17, 2163–2167
96 Reyzer, M.L. *et al.* (2003) Direct analysis of drug candidates in tissue by matrix-assisted laser desorption/ionization mass spectrometry. *J. Mass Spectrom.* 38, 1081–1092
97 Troendle, F.J. *et al.* (1999) Detection of pharmaceutical compounds in tissue by matrix-assisted laser desorption/ionization and laser desorption/chemical ionization tandem mass spectrometry with a quadrupole ion trap. *J. Am. Soc. Mass Spectrom.* 10, 1315–1321
98 Bunch, J. *et al.* (2004) Determination of pharmaceutical compounds in skin by imaging matrix-assisted laser desorption/ionisation mass spectrometry. *Rapid Commun. Mass Spectrom.* 18, 3051–3060
99 Behm, J.M. *et al.* (1996) Microscopic laser desorption postionization Fourier transform mass spectrometry. *Anal. Chem.* 68, 713–719
100 Sjovall, P. *et al.* (2004) Mass spectrometric imaging of lipids in brain tissue. *Anal. Chem.* 76, 4271–4278